J. Phycol. **46,** 1350–1355 (2010)
© 2010 Phycological Society of America
DOI: 10.1111/j.1529-8817.2010.00894.x

NOTE

MICROSENSOR MEASUREMENTS OF THE EXTERNAL AND INTERNAL MICROENVIRONMENT OF *FUCUS VESICULOSUS* (PHAEOPHYCEAE)[1]

Kristian Spilling[2]

Finnish Environment Institute, Marine Research Centre, PO Box 140, FIN-00250 Helsinki, Finland

Josefin Titelman

Department of Biology, University of Oslo, PO Box 1066 Blindern, N-0316 Oslo, Norway

Tina Maria Greve

Freshwater Biological Laboratory, Institute of Biology, University of Copenhagen, Helsingørgade 51, DK-3400 Hillerød, Denmark

and Michael Kühl

Marine Biological Laboratory, Department of Biology, University of Copenhagen, Strandpromenaden 5, DK-3000 Helsingør, Denmark

Plant Functional Biology and Climate Change Cluster, University of Technology Sydney, PO Box 123, Ultimo Sydney NSW 2007, Australia

We investigated the O_2, pH, and irradiance microenvironment in and around the tissue of the brown alga *Fucus vesiculosus* L. using microsensors. Microsensors are ideal tools for gaining new insights into what limits and controls macroalgal activity and growth at very fine spatial (<100 μm) and temporal (seconds) scales. This first microsensor investigation of a fucoid macroalga revealed differences in the microenvironment and metabolic activities at the level of different cell layers and thallus structures. *F. vesiculosus* responded quickly to rapid shifts in irradiance resulting in a highly dynamic microenvironment around and within its thallus. In combination with detailed morphological studies and molecular approaches, microsensors offer a promising toolbox to quantitatively describe structural and functional adaptations of macroalgae to environmental conditions, such as flow and light climate, as well as their physiological responses to environmental stressors.

Key index words: **boundary layer; brown algae, microsensor; oxygen gradients; photosynthesis, respiration**

Abbreviation: **DBL, diffusive boundary layer**

Primary productivity in communities of aquatic macrophytes varies with scale, and the organization of the community forms a canopy-like system that interacts with incident irradiance (Sand-Jensen et al. 2007). It remains unknown, however, if such scaling can be extrapolated to intratissue organization of photosynthetic units in aquatic macrophytes. The interplay between plant tissue structure and internal gradients of light and photosynthetic activity has been intensively studied in terrestrial plants (Smith et al. 1997, 2004), and a detailed understanding of relations between morphology, optics, and photosynthetic performance of terrestrial C3 plant leaves has been obtained (Vogelmann 1993, Richter and Fukshansky 1996a,b, 1998, Vogelmann et al. 1996). A similar understanding of aquatic plant tissue (e.g., macroalgal thalli and leaves of aquatic mosses, ferns, and angiosperms) is yet to be established (but see, e.g., Enriques and Sand-Jensen 2003). An important first step toward such a goal is to quantify the external and internal microgradients of key environmental and metabolic parameters in aquatic macrophytes.

Microsensor technology for chemical and optical measurements at <100 μm spatial resolution (reviewed in Revsbech and Jørgensen 1986, Kühl and Revsbech 2001, Kühl 2005) is well suited for such a purpose. Despite this, no direct measurements of the internal microenvironment of intact macroalgal tissues have been published, with the exception of two studies of green algae with relatively thick thalli: *Codium fragile* (Lassen et al. 1994) and *Halimeda discoidea* (de Beer and Larkum 2001). In this study, we explored the possibilities of using microsensors to describe interactions of external factors, such as light, flow, and tissue morphology, and their effect on the internal microenvironment and physiological processes of macroalgae. We demonstrate the applicability and potential of these

[1]Received 26 June 2009. Accepted 19 April 2010.
[2]Author for correspondence: e-mail kristian.spilling@environment.fi.

methods by presenting microprofiles of scalar irradiance, pigment fluorescence, O_2, and pH around and within tissue of the brown alga *F. vesiculosus*, along with measurements of photosynthesis and respiration under defined flow and irradiance regimes. The aim of this communication is not to test specific hypotheses of photosynthesis regulation, but rather to present the potential of microsensor technology for investigating microscale variation and regulation of photosynthesis and respiration in macroalgal tissues, and to point out directions for future studies of this underexplored research area within phycology.

Laboratory setup. *Fucus vesiculosus* specimens were collected from shallow (<2 m) waters in front of the Marine Station Rønbjerg, Denmark. A fresh piece of thallus (midapical part) was mounted in a plastic holder, which was positioned in a small flow chamber. The number of replicate thallus pieces used in different measurements is mentioned in the figure legends. The flow chamber was constantly flushed with water from a reservoir of aerated seawater at a free stream flow velocity of $\sim$1.5 cm $\cdot$ s^{-1}. Measurements were conducted under controlled light provided by a fiber-optic halogen lamp (Schott KL-2500, Mainz, Germany), which could be adjusted in color temperature and intensity.

The internal light field in the thallus was measured with scalar irradiance microprobes connected to a sensitive light meter and calibrated for measuring PAR (400–700 nm) (Kühl et al. 1997, Kühl 2005). The microprobes were inserted using a manually operated micromanipulator into the macroalgal tissue at a zenith angle of 135° relative to the vertically incident collimated light from the fiber-optic lamp. The <100 μm diameter spherical tip of the microprobe could not penetrate directly into the thallus, and it was necessary to make a tiny incision with the tip of a 30G hypodermic needle prior to insertion. For the same reason, we could only accomplish measurements in the medulla until the probe touched the lower cortex. Diffuse attenuation coefficients, $K_0(\mathrm{PAR})$, of quantum scalar irradiance, $E_0(\mathrm{PAR})$, over depth in the thallus, z, were determined in units of mm^{-1} as follows:

$$K_0(PAR) = -\frac{d\ln[E_0(PAR)]}{dz} = -\frac{\ln[E_0(PAR)_1/E_0(PAR)_2]}{z_2 - z_1} \quad (1)$$

where $E_0(\mathrm{PAR})_1$ and $E_0(\mathrm{PAR})_2$ are the quantum scalar irradiance measured at depths z_1 and z_2, respectively (Kühl 2005).

Microprofiles of chl *a* fluorescence (i.e., a proxy for photopigment distribution within the thallus) were measured across the thallus with 20–30 μm wide field radiance microprobes (Schreiber et al. 1996, Thar et al. 2001). Chl *a* at the fiber tip was excited with blue light (λ = 450–470 nm), and emitted fluorescence at λ > 665 nm was detected.

Clark-type O_2 microsensors (Revsbech 1989) with tip diameters of 10–25 μm were used to map the O_2 distribution and dynamics in the diffusive boundary layer (DBL) and within the thallus. For the latter measurements, it was necessary to use a 10 μm tip to avoid excessive compression and damage when entering the tissue. The sensors had a fast response time (t_{90} < 0.5 s). The O_2 microsensor was mounted on a motorized micromanipulator (LOT-Oriel GmbH, Märtzhäuser GmbH, Wetzlar, Germany) and connected to a pA meter (Unisense PA2000, Unisense A/S, Århus, Denmark). Microsensor signals were recorded both on a strip-chart recorder (Kipp and Zonen B.V., Delft, the Netherlands) and via PC-controlled data acquisition and microprofiling software (Profix, Unisense A/S, Århus, Denmark). The sensor was linearly calibrated from signal readings in O_2-free and in air-saturated seawater at experimental temperature, respectively. Oxygen concentrations were obtained from equations in Garcia and Gordon (1992). The microsensor tip position was defined relative to the upper level of the thallus, which was determined using a dissecting microscope (Zeiss SV6, Oberkochen, Germany) mounted on a boom stand. The measurement time for each sampling point, including movement of the sensor (50 μm) and stabilization of the measurement signal was 5–10 s. The measurement of a complete profile of O_2 concentration through the upper DBL, thallus, and the lower DBL (total of 3 mm in 50 μm increments) took $\sim$10 min.

The gross photosynthetic rate was measured at 50–100 μm spatial resolution by quantifying the rate of O_2 depletion during a brief light-dark shift (Revsbech and Jørgensen 1983). The spatial resolution of the method depends on the diffusion coefficient of O_2 in the tissue and on how precisely the initial O_2 depletion can be monitored with fast-responding O_2 microsensors. Typically, a spatial resolution of <100 μm can be realized when the O_2-depletion rate is determined over the first second after onset of darkness. In this study, measurements were done under varying irradiance with the microsensor tip positioned at the thallus surface, and at 50 μm depth increments through the thallus, which may thus show some overlap between measuring points. Net photosynthesis was estimated from measured steady-state O_2 microprofiles according to Revsbech and Jørgensen (1986) (see Appendix S1, in the supplementary material).

pH levels around the thallus were measured using a glass pH microsensor (Kühl and Revsbech 2001) and a standard calomel reference electrode (Radiometer A/S, Brønshøj, Denmark), which were both connected to a custom-built, high-impedance mV-meter. The pH-sensitive microsensor tip had a diameter of 10 μm and a length of 150 μm (including the leading nonresponsive fused glass tip),

yielding a spatial resolution of ~100 μm and a response time of 10–30 s. We positioned the pH microsensor as described for the O_2 sensor. The pH microsensors were calibrated at the experimental temperature in standard pH buffers (Radiometer A/S) of pH 4, 7, and 10.

Characterization of the microenvironment. *F. vesiculosus* exhibited fine-scale spatial patterns in the thallus microenvironment in all measured parameters (Figs. 1–3). While some of our results point toward specific adaptations in *F. vesiculosus* (see below), the main goal of this preliminary characterization of the microenvironments in *F. vesiculosus* was to demonstrate the applicability of microsensors to studies of thin macroalgal tissues. We were able to determine O_2-concentration microprofiles down to 50 μm spatial resolution, and fast O_2 dynamics upon experimental light-dark shifts. The pH sensor had a bit longer response time and was more sensitive to disturbance but could nonetheless produce reliable measurements of pH dynamics in the DBL. The methods presented here illustrate that microsensor analyses enable targeted studies of the dynamics and intratissue regulation of algal physiology over small spatial scales.

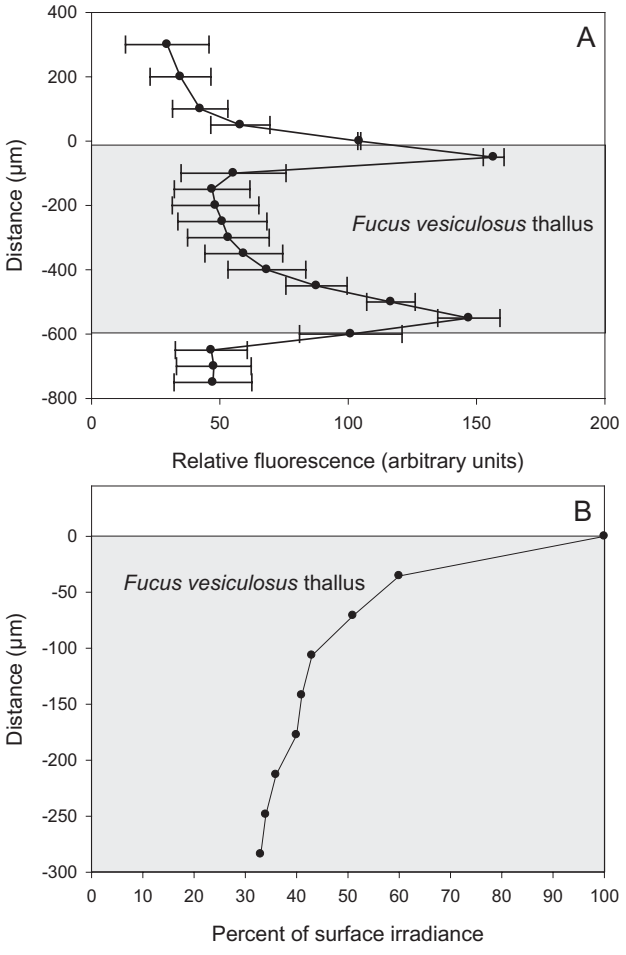

FIG. 1. (A) Microprofiles of chl *a* fluorescence in the thallus of *Fucus vesiculosus* (mean ± standard deviation, $n = 3$). (B) Quantum scalar irradiance in the thallus of *F. vesiculosus* ($n = 1$).

Light distribution. Cell density and chl *a* fluorescence were highest in the cortexes (Figs. 1 and S1 in the supplementary material), and PAR was strongly attenuated in the upper cortex, K_0(PAR) ~14 mm^{-1} (Fig. 1). Approximately 100 μm below the surface, <50% of the surface irradiance remained. Light attenuation in the medulla was much weaker, K_0(PAR) ~1.6 mm^{-1}, and the lower cortex received ~30% of the light incident at the upper surface.

The cellular organization of *F. vesiculosus* into cortex and medulla structurally resembles the palisade and mesophyll layers of terrestrial C3 plant leaves and might act similarly in light capturing. It has been speculated that medulla layers have light-guiding and optical properties linked to multiple scattering (Ramus 1978), and some experimental support exists for such phenomena in *Codium fragile* (Lassen et al. 1994). Detailed mapping of the internal light field (Vogelmann 1993, Kühl and Jørgensen 1994) is required to resolve how macroalgae optimize light capture. Fiber-optic microprobes (reviewed in Kühl 2005) are ideal tools for such studies.

Oxygen and pH dynamics. In concert with the light measurements (Fig. 1), we demonstrated considerable microscale spatial and temporal O_2 dynamics even within the apical parts. The highest net O_2 production recorded was 51 mmol $O_2 \cdot m^{-2} \cdot d^{-1}$ (Fig. S2 in the supplementary material), and in *F. vesiculosus*, the apical parts where we measured are the most productive regions (King and Schramm 1976). Vertically through the thallus, the O_2 concentration was highest in the medulla during illumination, while the upper and lower cortex had the highest photosynthetic production (Fig. 2). The apparent drop in O_2 concentration in the lower cortex (Fig. 2) was probably due to the sensor pushing on the lower cortex on its way out. Oxygen produced in cortex layers diffused both toward the surrounding water through the DBL and into the medullae tissue in the thallus. The O_2 transport properties of the medulla remain unknown but are apparently governed by slower lateral O_2 transport by diffusion. The O_2 levels and gross photosynthesis rates in the thallus varied with irradiance. At low-moderate light levels, the upper cortex exhibited highest photosynthetic activity due to the strong light attenuation across the thallus. This light limitation was alleviated at higher irradiance, where both upper and lower cortex displayed high activities and supersaturation of O_2 throughout the thallus. Adding the production in upper and lower cortex (by splitting the data in the middle of medulla) revealed that the lower cortex had only ~7% lower production at high light intensities, suggesting a rapid light acclimation. The apparent asymmetry in thickness of the O_2 production in the two cortexes (Fig. 2) is probably due to measurement uncertainty (e.g., by

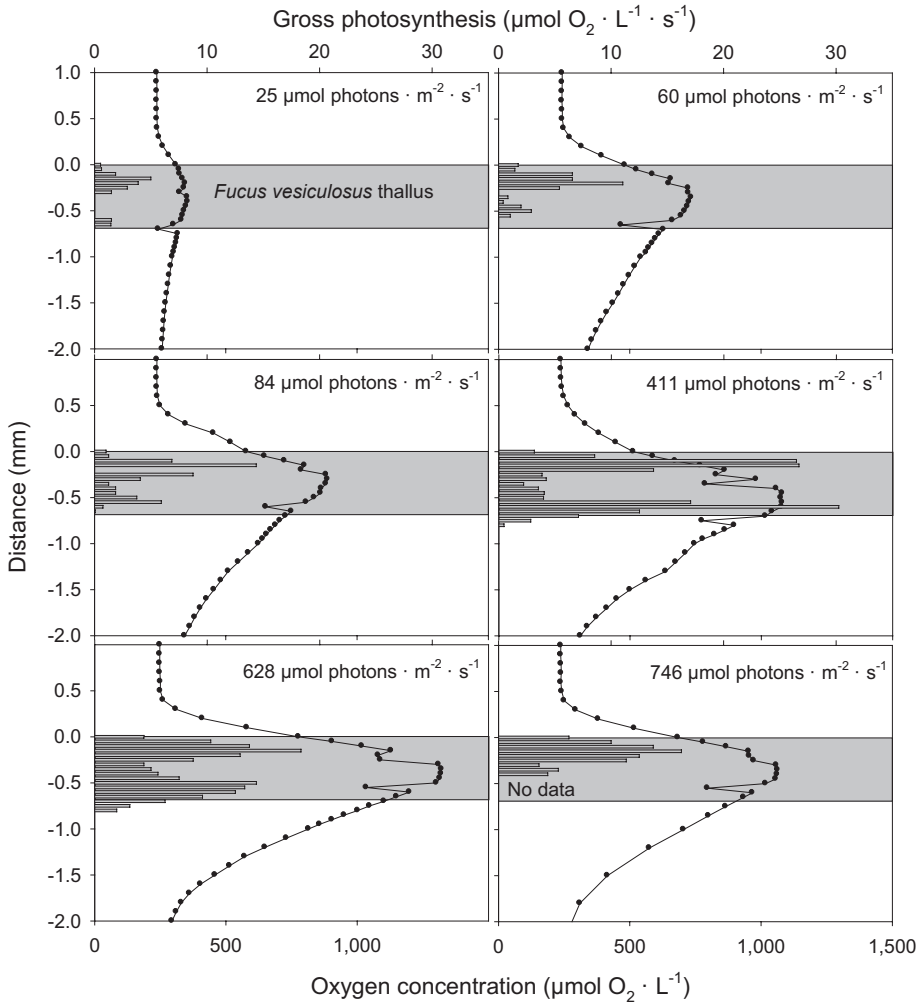

FIG. 2. Oxygen profiles (filled circles) through the thallus and the surrounding diffusive boundary layers, and gross photosynthesis (bars) measured as a function of increasing irradiance. The gray box indicates the thallus position. All the measurements were done via the same insertion point ($n = 1$).

thallus compression when measuring in deeper layers), as sections of the thallus showed the same thickness of the upper and lower cortexes (Fig. S1). Microenvironmental analysis of macroalgae may provide insights into specific functions. For example, the effect of the elevated pH at the thallus surface during photosynthesis (Fig. 3) may represent a rate-limiting step in primary production due to carbon limitation (Riebesell et al. 1993, Larkum et al. 2003) or changes in membrane transport and internal pH (Smith and Raven 1979). Macroalgal tolerance of high pH is species-specific (Menéndez et al. 2001), but pH >8.6 lowers primary production in many marine autotrophs (Riebesell et al. 1993, Menéndez et al. 2001).

Measurements on the surface of a dark-acclimated thallus revealed rapidly increasing O_2 concentration and pH due to photosynthesis after onset of illumination (Fig. S3 in the supplementary material). The level of O_2 and pH at the thallus surface increased

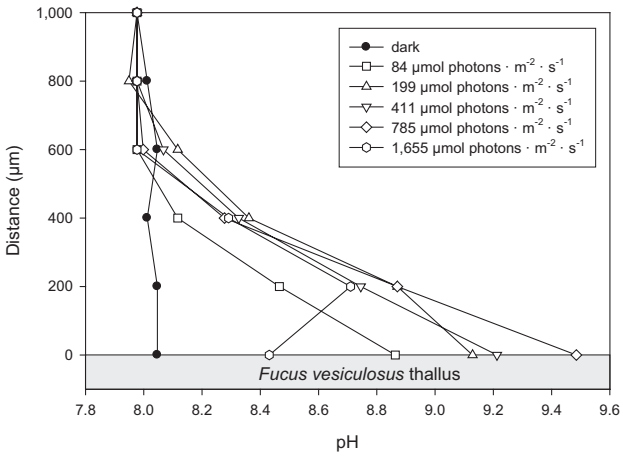

FIG. 3. Examples of pH microprofiles measured through the diffusive boundary layer toward the thallus surface as a function of increasing irradiance (color temperature: 3,050 K). Measurements were conducted in the dark (solid symbols) and varying light conditions (open symbols) on the same thallus ($n = 1$).

with irradiance, reaching the highest levels of pH (9.5) and O_2 levels of >1 mM (Figs. 2 and 3). The temporal resolution and quick response time in these measurements pinpoints the applicability of these methods in targeted examinations of dynamic processes in and with the DBL, which depending on flow rate, may rapidly produce mass transfer limitations (Larkum et al. 2003, Stewart and Carpenter 2003).

We also attempted comparative O_2 microprofiling in smooth thallus parts and across patches of hyaline hairs rooted in cryptostomata (Fig. S4 in the supplementary material). The cryptostomata cavity examined displayed reduced fluorescence, different O_2 dynamics (Figs. 2 and S4), and a thicker DBL (Table 1) than the surrounding tissue. The net O_2 production was ~35% lower, and dark respiration rate was ~70% higher in the cryptosomata. In darkness, the cryptostomata cavity approached anoxia (<7 μmol $O_2 \cdot L^{-1}$, <3% air saturation), which could potentially provide an environment for anoxic microbial processes (Gerard et al. 1990). The O_2 content in normal thallus tissue was always >60 μmol $O_2 \cdot L^{-1}$ (~27% air saturation). Although we lack sufficient replication to conclude that the observed differences between tissues can be generalized, we hypothesize that there can be considerable horizontal variation in metabolic activity on a very small spatial scale within a thallus. The thicker DBL over cryptostomata was presumably due to their rougher surface topography with hyaline hairs (Fig. S1 and Table 1). The role of hyaline hairs and the DBL thickness is unresolved but may be related to nutrient uptake (Hurd et al. 1993, Steen 2003). A thicker DBL reduces mass transport, resulting in slower nutrient uptake. However, a thicker DBL may also increase efficiency of nutrient-transforming surface enzymes (Raven 1992, Hurd 2000). Individual hairs reaching into the water may experience a thinner DBL, enhancing local nutrient uptake (Raven 1981, Hurd 2000). Our measurements were conducted with moderate and uniform flow, but flow can significantly affect solute exchange across the DBL (Larkum et al. 2003), and extrapolation to in situ flow effects is difficult. Clearly, the mechanistic interactions between flow, solute exchange, and primary production in macroalgae (Stewart and Carpenter 2003) on small spatial scales deserves further attention, as does the functional role of specific macroalgal morphologic structures. Microsensor measurements can provide fundamental insight into such processes.

Table 1. Differences in diffusive boundary layer (DBL) thickness, respiration, maximum net primary production (P_m-net), and maximum and minimum oxygen concentration between a cryptostomata cavity and normal thallus tissue situated ~10 mm apart. The corresponding oxygen profiles are depicted in Figure S3 (in the supplementary material).

	Normal thallus tissue	Cryptostomata
DBL thickness (μm)	500	800
Respiration (mmol $O_2 \cdot m^{-2} \cdot d^{-1}$)	−4.5	−7.6
P_m-net (mmol $O_2 \cdot m^{-2} \cdot d^{-1}$)	25.9	16.8
O_2 max (μmol $O_2 \cdot L^{-1}$)	1,096	860
O_2 min (μmol $O_2 \cdot L^{-1}$)	65.6	6.5

Conclusion. Microsensors are ideal tools for gaining new insights into what limits and controls macroalgal activity and growth at very fine spatial and temporal scales. This first microsensor investigation of a fucoid macroalga revealed differences in the microenvironment and metabolic activities at the level of different cell layers and thin thallus structures. *F. vesiculosus* responded quickly to rapid shifts in irradiance, resulting in a highly dynamic microenvironment around and within its thallus. In combination with detailed morphological studies and new imaging methods (Kühl and Polerecky 2008), microsensors offer a promising toolbox to quantitatively describe structural and functional adaptations of macroalgae to environmental conditions such as flow and light climate, as well as their physiological responses to environmental stressors. Such studies are currently lacking in phycology and could find strong inspiration in microscale studies of terrestrial plant tissues (Vogelmann et al. 1996). In terms of studying the chemical dynamics, microscale measurements in aquatic macrophytes are relatively easier to perform than in terrestrial plants due to the much (~10^4 times) slower diffusion of key variables like O_2 and CO_2 in water as compared to air, allowing the build up of pronounced gradients and a more dynamic microenvironment.

This study was conducted during the Ph.D. course Microsensor Analysis in the Environmental Sciences, which was funded by the Nordic Academy for Advanced Study (NorFA) (M. K.). Additional support was received from Walter and Andreè de Nottbeck foundation (K. S.) and the Danish Natural Science Research Council (M. K.). We thank Anni Glud for excellent technical assistance and microsensor construction, Bob Hund for inspiration, and Unisense A/S for providing oxygen microsensors and measuring equipment.

de Beer, D. & Larkum, A. W. D. 2001. Photosynthesis and calcification in the calcifying algae *Halimeda discoidea* studied with microsensors. *Plant Cell Environ.* 24:1209–18.

Enriques, S. & Sand-Jensen, K. 2003. Variation in light absorption properties of *Mentha aquatica* L. as a function of leaf form: implications for plant growth. *Int. J. Plant Sci.* 164:125–36.

Garcia, H. E. & Gordon, L. I. 1992. Oxygen solubility in seawater: better fitting equations. *Limnol. Oceanogr.* 37:1307–12.

Gerard, V. A., Dunham, S. E. & Rosenberg, G. 1990. Nitrogen fixation by cyanobacteria associated with *Codium fragile* (Chlorophyta): environmental effects and transfer of fixed nitrogen. *Mar. Biol.* 105:1–8.

Hurd, C. L. 2000. Water motion, marine macroalgal physiology, and production. *J. Phycol.* 36:453–72.

Hurd, C. L., Galvin, R. S., Norton, T. A. & Dring, M. J. 1993. Production of hyaline hairs by intertidal species of *Fucus* (Fucales) and their role in phosphate uptake. *J. Phycol.* 29:160–5.

King, R. J. & Schramm, W. 1976. Determination of photosynthetic rates for the marine algae *Fucus vesiculosus* and *Laminaria digitata*. *Mar. Biol.* 37:209–13.

Kühl, M. 2005. Optical microsensors for analysis of microbial communities. *Methods Enzymol.* 397:166–99.
Kühl, M. & Jørgensen, B. B. 1994. The light field of micro-benthic communities: radiance distribution and microscale optics of sandy coastal sediments. *Limnol. Oceanogr.* 39:1368–98.
Kühl, M., Lassen, C. & Revsbech, N. P. 1997. A simple light meter for measurements of PAR (400 to 700 nm) with fiber-optic microprobes: application for P vs. E_0 (PAR) measurements in a microbial mat. *Aquat. Microb. Ecol.* 13:197–207.
Kühl, M. & Polerecky, L. 2008. Functional and structural imaging of phototrophic microbial communities and symbioses. *Aquat. Microb. Ecol.* 53:99–118.
Kühl, M. & Revsbech, N. P. 2001. Biogeochemical microsensors for boundary layer studies. *In* Boudreau, B. P. & Jørgensen, B. B. [Eds.] *The Benthic Boundary Layer.* Oxford University Press, Oxford, UK, pp. 180–210.
Larkum, A. W. D., Koch, E. M. & Kühl, M. 2003. Diffusive boundary layers and photosynthesis of the epilithic algal community of coral reefs. *Mar. Biol.* 142:1073–82.
Lassen, C., Bebout, L. E., Pearl, H. W. & Jørgensen, B. B. 1994. Microsensor studies of oxygen distribution in the green macroalgae *Codium fragile. J. Phycol.* 30:381–6.
Menéndez, M., Martinez, M. & Comin, F. A. 2001. A comparative study of the effect of pH and inorganic carbon resources on the photosynthesis of three floating macroalgae species of a Mediterranean coastal lagoon. *J. Exp. Mar. Biol. Ecol.* 256: 123–36.
Ramus, J. 1978. Seaweed anatomy and photosynthetic performance: the ecological significance of light guides, heterogeneous absorption and multiple scatter. *J. Phycol.* 14: 352–62.
Raven, J. A. 1981. Nutritional strategies of submerged benthic plants: the acquisition of C, N and P by rhizophytes and haptophytes. *New Phytol.* 88:1–30.
Raven, J. A. 1992. How benthic macroalgae cope with flowing water: resource acquisition and retention. *J. Phycol.* 28:133–46.
Revsbech, N. P. 1989. An oxygen microelectrode with a guard cathode. *Limnol. Oceanogr.* 34:474–8.
Revsbech, N. P. & Jørgensen, B. B. 1983. Photosynthesis of benthic microflora measured by the oxygen microprofile method: capabilities and limitations of the method. *Limnol. Oceanogr.* 28:749–56.
Revsbech, N. P. & Jørgensen, B. B. 1986. Microelectrodes: their use in microbial ecology. *Adv. Microb. Ecol.* 9:293–352.
Richter, T. & Fukshansky, L. 1996a. Optics of a bifacial leaf. 1. A novel combined procedure for deriving the optical parameters. *Photochem. Photobiol.* 63:507–16.
Richter, T. & Fukshansky, L. 1996b. Optics of a bifacial leaf. 2. Light regime as affected by the leaf structure and the light source. *Photochem. Photobiol.* 63:517–27.
Richter, T. & Fukshansky, L. 1998. Optics of a bifacial leaf. 3. Implications for photosynthetic performance. *Photochem. Photobiol.* 68:337–52.
Riebesell, U., Wolf-Gladrow, D. A. & Smetacek, V. 1993. Carbon dioxide limitation of marine phytoplankton growth rates. *Nature* 361:249–51.
Sand-Jensen, K., Binzer, T. & Middelboe, A. L. 2007. Scaling of photosynthetic production of aquatic macrophytes – a review. *Oikos* 116:280–94.
Schreiber, U., Kühl, M., Klimant, I. & Reising, H. 1996. Measurement of chlorophyll fluorescence within leaves using a modified PAM fluorometer with a fiber-optic microprobe. *Photosynth. Res.* 47:103–9.
Smith, F. & Raven, J. A. 1979. Intracellular pH and its regulation. *Ann. Rev. Plant Physiol.* 30:289–311.
Smith, W. K., Vogelmann, T. C. & Critchley, C. [Eds.] 2004. *Photosynthetic Adaptation: Chloroplast to Landscape.* Ecological Studies 178. Springer, New York, 309 pp.
Smith, W. K., Vogelmann, T. C., DeLucia, E. H., Bell, D. T. & Shepherd, K. A. 1997. Leaf form and photosynthesis. *Bioscience* 47:785–93.
Steen, H. 2003. Apical hair formation and growth of *Fucus evanescens* and *F. serratus* (Phaeophyceae) germlings under various nutrient and temperature regimes. *Phycologia* 42: 26–30.
Stewart, H. L. & Carpenter, R. C. 2003. The effects of morphology and water flow on photosynthesis of marine macroalgae. *Ecology* 84:2999–3012.
Thar, R., Kühl, M. & Holst, G. 2001. A fiber-optic fluorometer for microscale mapping of photosynthetic pigments in microbial communities. *Appl. Environ. Microbiol.* 67:2823–8.
Vogelmann, T. C. 1993. Plant tissue optics. *Ann. Rev. Plant Physiol. Plant Mol. Biol.* 44:231–51.
Vogelmann, T. C., Nishio, J. N. & Smith, W. K. 1996. Leaves and light capture: light propagation and gradients of carbon fixation within leaves. *Trends Plant Sci.* 1:65–71.

Supplementary Material

The following supplementary material is available for this article:

Figure S1. Cross-section of *Fucus vesiculosus* thallus showing the cryptostomata cavity and hyaline hairs. Scale bar, 500 μm.

Figure S2. O_2 microprofiles in the diffusive boundary layer (A) and the net O_2 production versus irradiance (B) of *Fucus vesiculosus*. The net production was calculated using equation S1 (see methods in Appendix S1 for equations). The solid line in (B) represents the nonlinear curve fit of equation S2 to the net production, and E_k was calculated according to equation S3. E_c is the compensation point in μmol photons $\cdot$ $m^{-2} \cdot s^{-1}$.

Figure S3. Oxygen concentration (○) and pH (▽) measured at the surface of the *Fucus vesiculosus* thallus in darkness (black symbols), at the onset of illumination (gray symbols), and after onset of illumination (open symbols). Irradiance was ~500 μmol photons $\cdot$ $m^{-2} \cdot s^{-1}$ ($n = 2$, error bars indicate standard deviation).

Figure S4. Oxygen microprofiles measured through thallus and cryptostomata in darkness and at saturating irradiance (~500 μmol photons $\cdot$ $m^{-2} \cdot s^{-1}$). The two points were measured ~10 mm apart. Calculations of P_m and respiration are presented in Table 1.

Appendix S1. Methods.

This material is available as part of the online article.

Please note: Wiley-Blackwell are not responsible for the content or functionality of any supporting materials supplied by the authors. Any queries (other than missing material) should be directed to the corresponding author for the article.